Collective excitations in a spin-polarized quasi-two-dimensional electron gas

J. C. Ryan
Naval Research Laboratory, Washington, D.C. 20375
(Received 9 October 1990)

The dispersion relations of the collective modes of an optically created two-dimensional spin-polarized electron plasma, treated as a confined spin-polarized electron gas, are calculated. These exhibit many significant qualitative differences from their spin-unpolarized counterparts, such as emergence of the intrasubband spin wave and splitting of the intersubband spin waves and the longitudinal spin-density oscillations.

In recent years there has been much work on the excitation spectra of the quasi-two-dimensional (quasi-2D) electron gas. Although there have been some notable exceptions,[1] most of the work includes electron-electron interactions within the context of the random-phase approximations (RPA), thereby neglecting the exchange and correlation contributions to the interaction.

The only collective excitations possible within the RPA are various types of plasmons. However, when exchange and correlation aspects of the interaction are included, there can also be collective spin density oscillations. In general there will be longitudinal spin-density modes, which may couple to the plasmon modes, and transverse modes, which involve a spin flip. For conventional quasi-2D systems [silicon metal-oxide semiconductor field-effect transistor (MOSFET's), GaAs quantum wells, etc.] there will be no spin polarization, and thus no preferred direction to distinguish longitudinal from transverse. The longitudinal and transverse modes become degenerate and uncoupled from the plasmon modes.

Spin polarization can be created by pumping an undoped quantum well with circularly polarized light.[2] This will selectively excite a single spin species resulting in a spin-polarized plasma. Although such a system will be more complicated than the degenerate spin-polarized gas presented here, the effects of the hole plasma can be incorporated when bound excitonic effects are suppressed.

The ferromagnetic state of a 2D electron gas has been examined by Rajagopal and co-workers.[3,4] Although the existence of such a state remains an open question in real 2D systems, it is suggested here that the optically induced plasma be treated as a confined spin-polarized electron gas.

In this paper we examine the effect of spin-polarization on the collective modes of the quasi-2D electron gas with exchange and correlation included through the local-spin-density approximation (LSDA). The LSDA is an approximation to the spin-density functional theory in which the energy functional is considered to depend only upon the spinor density, and not on any of its derivatives. The LSDA is only rigorously justified if the density does not vary significantly over the radius of the exchange and correlation hole; however, it has been shown to give surprisingly good results for many nonhomogeneous systems,[5] including the single quantum well.[6] This approach is essentially a mean-field approximation to the many-body problem, with the exchange and correlation contribution to the mean-field potential (known as the Hohenberg-Kohn-Sham potential) being of the point-contact type in the LSDA.

Collective excitations appear as poles in the various linear response functions. In general these excitations will be damped at all energies, however, within the approximations made here they will only be damped when they enter the continuum of quasi-particle-hole excitations.

The linear-response functions, in the LSDA, for an arbitrary electron system have been derived by Rajagopal.[7] We apply this theory to a quasi-2D electron system by expanding the creation-annihilation operators in the LSDA quasi-particle states appropriate to the particular system. In the effective-mass approximation

$$\psi_\alpha(\mathbf{x})=\sum_{n,\mathbf{k}}\frac{e^{i\mathbf{k}\cdot\mathbf{r}}}{A^{1/2}}\xi_a(z)c_{\alpha n\mathbf{k}}\ , \tag{1}$$

where the confinement in the z direction is due to Bragg reflection, dielectric images, impurity potentials, applied bias fields, etc., and the state indices n can be either discrete, as in a quantum well (QW) or MOSFET, or continuous as in a superlattice. The response functions in subband space obey the equation

$$\begin{aligned}\Pi_{nmm'n'}(\mathbf{q},\omega)\\ &=\Pi^0_{nm}(\mathbf{q},\omega)\delta_{nn'}\delta_{mm'}\\ &\quad+\Pi^0_{nm}(\mathbf{q},\omega)\sum_{n''m''}\delta\Sigma_{mnn''m''}(\mathbf{q})\Pi_{n''m''m'n'}(\mathbf{q},\omega)\ ,\end{aligned} \tag{2}$$

where each element of the subband matrix is a 4×4 partitioned spin matrix and $\Pi^0_{nm}(\mathbf{q},\omega)$ is the polarizability of the noninteracting quasiparticles. The same result could be obtained from a diagrammatic approach if the four-point interaction in the irreducible vertex equation is replaced by an effective point-contact interaction.

To illustrate the effects of broken spin symmetry we will concentrate on the simplest quasi-2D system, a single quantum well. Thus we will not deal with the more complex matrix structure in the Hilbert space of states necessary to handle other systems such as multiple quantum wells or superlattices.

For a single quantum well the eigenvalues are nondegenerate and denoted by the set of integers in the desired energy range. The subband summation in Eq. (2) is discrete, with the interaction matrix elements defined by

$$\delta\Sigma_{mnn'm'}(\mathbf{q}) = \int dz\, dz' \xi_n(z)\xi_m(z)\frac{2\pi e^2}{\epsilon q}e^{-q|z-z'|}\xi_{n'}(z')\xi_{m'}(z') + \int dz\, \xi_n(z)\xi_m(z)\delta\Sigma^{xc}(n(z))\xi_{n'}(z)\xi_{m'}(z) . \tag{3}$$

The matrix elements of the noninteracting polarizabilities are

$$[\Pi^0_{nm}(\mathbf{q},\omega)]_{\alpha\beta} = \int \frac{d^2k}{(2\pi)^2}\frac{f_\alpha(\omega_n(\mathbf{k}+\mathbf{q}/2))-f_\beta(\omega_m(\mathbf{k}-\mathbf{q}/2))}{\omega_n(\mathbf{k}+\mathbf{q}/2)-\omega_m(\mathbf{k}-\mathbf{q}/2)-\omega} , \tag{4}$$

where the greek indices denote spin.

The spin structure can be simplified by expressing the response functions in terms of the Pauli matrices as in Ref. 6 (suppressing subband indices)

$$\Pi_{ij} = \sum_{\alpha\beta\beta'\alpha'} \sigma^i_{\alpha\beta}\Pi_{\alpha\beta\beta'\alpha'}\sigma^j_{\alpha'\beta'} \tag{5}$$

from which we obtain block diagonals of 1×1, 1×1, and 2×2, for the transverse and longitudinal modes, respectively.

We further specialize this to a symmetric well in which only the lowest subband is occupied and consider only excitations within the lowest two subbands. In this case the intrasubband excitations, in which all quasiparticle transitions are within the ground subband, and intersubband excitations, which involve transitions to the next higher subband, are uncoupled. The subband matrix is diagonalized by transforming to a function χ_{ij} which is equal to $[\Pi_{0000}]_{ij}$ for intrasubband and $[\Pi_{1001}+\Pi_{1010}+\Pi_{0101}+\Pi_{0110}]_{ij}$ for intersubband contributions. It follows that both inter- and intrasubband contributions to the response functions are of the form

$$\chi_{00}=D^{-1}\left[\chi^0_+ - \left\langle\frac{\partial^2\varepsilon^{xc}}{\partial s^2}\right\rangle(\chi^{0\,2}_+-\chi^{0\,2}_-)\right] , \tag{6a}$$

$$\chi_{33}=D^{-1}\left[\chi^0_+ - \left\langle V_h+\frac{\partial^2\varepsilon^{xc}}{\partial n^2}\right\rangle(\chi^{0\,2}_+-\chi^{0\,2}_-)\right] , \tag{6b}$$

$$\chi_{03}=\chi_{30}=D^{-1}\left[\chi^0_- + \left\langle\frac{\partial^2\varepsilon^{xc}}{\partial s\,\partial n}\right\rangle(\chi^{0\,2}_+-\chi^{0\,2}_-)\right] \tag{6c}$$

for the longitudinal response, where

$$D = \left[1-\chi^0_+\left\langle\frac{\partial^2\varepsilon^{xc}}{\partial s^2}\right\rangle-\chi^0_-\left\langle\frac{\partial^2\varepsilon^{xc}}{\partial s\,\partial n}\right\rangle\right]\left[1-\chi^0_+\left\langle V_h+\frac{\partial^2\varepsilon^{xc}}{\partial n^2}\right\rangle-\chi^0_-\left\langle\frac{\partial^2\varepsilon^{xc}}{\partial s\,\partial n}\right\rangle\right] - \left[\chi^0_-\left\langle\frac{\partial^2\varepsilon^{xc}}{\partial s^2}\right\rangle+\chi^0_+\left\langle\frac{\partial^2\varepsilon^{xc}}{\partial s\,\partial n}\right\rangle\right]\left[\chi^0_-\left\langle V_h+\frac{\partial^2\varepsilon^{xc}}{\partial n^2}\right\rangle+\chi^0_+\left\langle\frac{\partial^2\varepsilon^{xc}}{\partial s\,\partial n}\right\rangle\right] \tag{7}$$

and

$$\chi_{-+}=4\chi^0_{\downarrow\uparrow}\left[1-\chi^0_{\downarrow\uparrow}\left\langle\frac{2}{s}\frac{\partial\varepsilon^{xc}}{\partial s}\right\rangle\right]^{-1} , \quad \chi_{+-}=4\chi^0_{\uparrow\downarrow}\left[1-\chi^0_{\uparrow\downarrow}\left\langle\frac{2}{s}\frac{\partial\varepsilon^{xc}}{\partial s}\right\rangle\right]^{-1} \tag{8}$$

for the transverse response. Here $\chi^0_{\alpha\beta}$ (with wave-vector and energy units the inverse Bohr radius and Rydberg in the material, respectively) and $\langle\delta\Sigma\rangle$ are

$$\chi^0_{\alpha\beta}=[\Pi^0_{10}(\mathbf{q},\omega)+\Pi^0_{01}(\mathbf{q},\omega)]_{\alpha\beta} = -\frac{1}{\pi q^2}\{2\omega_{10}+2q^2+[(\omega+\omega_{10}+q^2)^2-(2k_{F\alpha}q)^2]^{1/2}-\mathrm{sgn}(\omega-\omega_{10}-q^2)[(\omega-\omega_{10}-q^2)^2-(2k_{F\beta}q)^2]^{1/2}\} \tag{9}$$

and $\langle\delta\Sigma\rangle=\delta\Sigma_{0101}$ for the intersubband modes, and

$$\chi^0_{\alpha\beta}=[\Pi^0_{00}(\mathbf{q},\omega)]_{\alpha\beta}=\lim_{\omega_{10}\to0}[\Pi^0_{10}(\mathbf{q},\omega)+\Pi^0_{01}(\mathbf{q},\omega)]_{\alpha\beta} \tag{10}$$

and $\langle\delta\Sigma\rangle=\delta\Sigma_{0000}$ for intrasubband modes, where ω_{10} is the intersubband energy, $k_{F\alpha}$ is the Fermi wave vector for spin α electrons, ε^{xc} is the energy density, and $\chi^0_\pm$ is defined as

$$\chi^0_+=\chi^0_{\uparrow\uparrow}+\chi^0_{\downarrow\downarrow}, \quad \chi^0_-=\chi^0_{\uparrow\uparrow}-\chi^0_{\downarrow\downarrow} . \tag{11}$$

In the paramagnetic limit for $s\to0$,

$$\Pi^0_{\uparrow\uparrow}=\Pi^0_{\downarrow\downarrow}=\Pi^0_{\uparrow\downarrow}=\Pi^0_{\downarrow\uparrow} \tag{12}$$

for all subband indices and

$$\frac{\partial\varepsilon^{xc}}{\partial s}\approx s\left.\frac{\partial^2\varepsilon^{xc}}{\partial s^2}\right|_{s=0}\to0 \tag{13}$$

which yields $\chi_{-+}=\chi_{+-}=2\chi_{33}$ and $\chi_{03}=0$, thus we recover the results of Ref. 5 in this limit.

We now present a simple model of the single quantum well (SQW) to illustrate the above results. We choose the envelope functions to be cosine and sine functions,

$$\xi_0(z)=(2k/\pi)^{1/2}\cos kz, \quad \xi_1(z)=(2k/\pi)^{1/2}\sin 2kz \tag{14}$$

with the well width chosen so that the subband energy spacing in GaAs will be 15.5 meV. We also use an area density of 3.6×10^{11} cm^{-2}. These numbers are appropriate for the experimental set up in Ref. 5. The correlation contribution to the energy is neglected and hence

$$\varepsilon^x=-\frac{3}{4}\left[\frac{3}{\pi}\right]^{1/3}\{[n(z)+s(z)]^{4/3}+[n(z)-s(z)]^{4/3}\} . \tag{15}$$

We also assume that the spin polarization is proportional to the density

$$s(z)=\zeta n(z) \tag{16}$$

so that

$$\frac{\partial^2\varepsilon^{xc}}{\partial n^2}=\frac{\partial^2\varepsilon^{xc}}{\partial s^2}=-E_0(z)\frac{[(1+\zeta)^{-2/3}+(1-\zeta)^{-2/3}}{2} , \tag{17a}$$

$$\frac{\partial^2\varepsilon^{xc}}{\partial s\,\partial n}=-E_0(z)\frac{[(1+\zeta)^{-2/3}-(1-\zeta)^{-2/3}]}{2} , \tag{17b}$$

$$\frac{1}{s}\frac{\partial\varepsilon^{xc}}{\partial s}=-E_0(z)\frac{3[(1+\zeta)^{1/3}-(1-\zeta)^{1/3}]}{2\zeta} , \tag{17c}$$

$$E_0(z)=\frac{2}{3}\left[\frac{3}{\pi}\right]^{1/3}[n(z)]^{-2/3} , \tag{18}$$

where ζ takes on values between 0 and 1, and will be determined by the laser intensity and relaxation rates.

Evaluating the matrix elements of the exchange and Hartree terms we find

$$\langle E_0(z)\rangle_{0000}=5\left[\frac{3k}{2\pi^2 n_s^2}\right]^{1/3}\frac{\Gamma(\frac{2}{3})}{[\Gamma(\frac{1}{3})]^2} , \tag{19a}$$

$$\langle V_h\rangle_{0000}=\frac{4}{q}\left[\frac{2k}{q}+\frac{kq}{q^2+4k^2}-\frac{32k^2}{\pi q^2}\frac{(1-e^{-\pi q/k})}{(q^2+4k^2)^2}\right] \tag{19b}$$

for the intrasubband modes, and

$$\langle E_0(z)\rangle_{0101}=\frac{30}{7}\left[\frac{3k}{2\pi^2 n_s^2}\right]^{1/3}\frac{\Gamma(\frac{2}{3})}{[\Gamma(\frac{1}{3})]^2} , \tag{20a}$$

$$\langle V_h\rangle_{0101}=4k\left[\frac{1}{q^2+k^2}+\frac{1}{q^2+9k^2}-\frac{2kq}{\pi}(1+e^{-\pi q/k})\times\left[\frac{1}{q^2+k^2}-\frac{1}{q^2+9k^2}\right]^2\right] . \tag{20b}$$

for the intersubband modes.

In Fig. 1 we plot the nondamped collective modes at zero in-plane momentum as a function of spin polarization, with the intersubband energy denoted by the dotted line. The mode labeled L_1 is known as the intersubband plasmon at $\zeta=0$. The mode position does not change significantly with ζ; however, at nonzero ζ the longitudi-

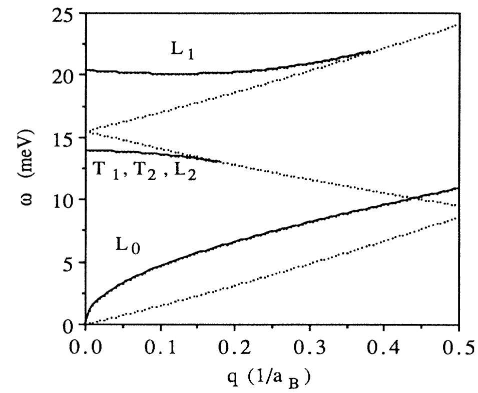

FIG. 2. Frequencies of the collective modes vs q at $\zeta=0.0$.

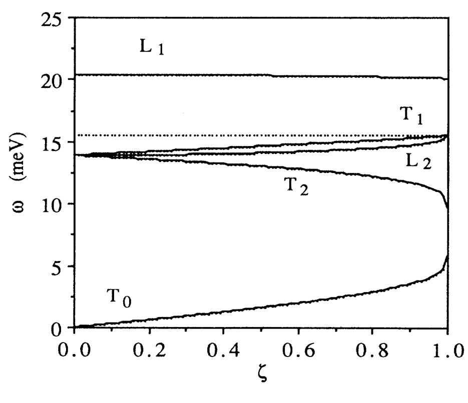

FIG. 1. Frequencies of the collective modes vs ζ at $q=0$.

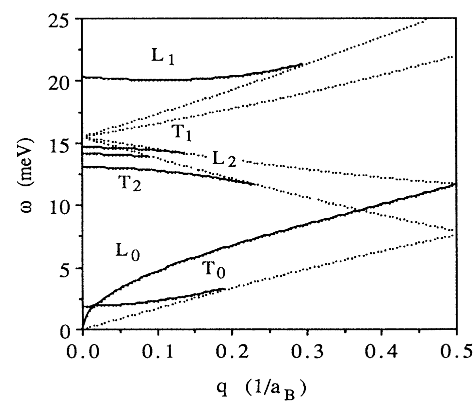

FIG. 3. Frequencies of the collective modes vs q at $\zeta=0.5$.

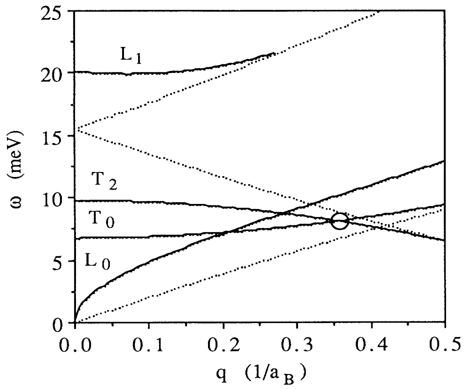

FIG. 4. Frequencies of the collective modes vs q at $\zeta=1.0$.

nal modes can no longer be characterized as charge and spin-density modes, but rather of mixed character with the mixing determined by χ_{03}, such that the spin and charge-density coupling becomes equal at $\zeta=1$ ($\chi_{03}=\chi_{00}=\chi_{33}$).

The other longitudinal mode, L_2, and the two transverse modes, T_1 and T_2, are degenerate at $\zeta=0$. The spin-down to spin-up mode, T_1 (pole of χ_{-+}) and L_2 both approach the intersubband energy with vanishing strength at $\zeta=1$, while the T_2 mode (pole of χ_{+-}) remains finite. Both the T_1 and L_2 modes disappear because there are no spin-down electrons.

The lower-energy mode, denoted T_0, is the intrasubband spin wave, which vanishes at $\zeta=0$. Another undamped mode that does not appear in Fig. 1 is the longitudinal intrasubband mode L_0, whose frequency varies as $q^{1/2}$ for small q, and thus will not be seen at $q=0$. The remaining intrasubband modes will lie in the particle-hole continuum for all q.

In Figs. 2–4 the respective dispersion relations for values of $\zeta=0.0$, 0.5, and 1.0 are plotted, showing the appearance of the L_0 mode for $q\neq0$. The dotted lines indicate the boundaries of the particle-hole continuum. At $\zeta=0.0$ the intersubband plasmon and the spin-density modes can be seen merging with the intersubband continuum; the intrasubband mode L_0, will merge with the intrasubband continuum at a higher value of q. At $\zeta=0.5$ the degenerate modes split and the intrasubband spin wave emerges from the continuum. The extra dotted lines represent the nondegenerate spin-up and spin-down continua. And finally at $\zeta=1.0$ the T_1 and L_2 modes, and the spin-down continuum disappear.

The circle in Fig. 4 marks the intersection of the inter- and intrasubband spin waves. If there were an asymmetry in the well the inter- and intrasubband modes would couple and this crossing would become an anticrossing. There would also be damping of the intrasubband modes in the intersubband continuum, and vice versa. The other crossing points are between longitudinal and transverse modes, which will not couple.

A direct observation of the collective modes is often made through Raman scattering. The transverse or spin-flip modes will only be visible in the cross-polarized spectra. However, due to the mixed spin-charge character of the longitudinal modes at nonzero polarization, both longitudinal modes will appear in the polarized and cross-polarized Raman spectra.

Another consequence of the broken spin symmetry will appear as a coupling of the collective modes to phonons. Although the presence of phonons was not incorporated in the present work, it is evident that a LO phonon mode and the L_1 mode will couple only at nonzero spin polarization, due to the loss of charge neutrality of the L_2 mode.

In this paper we have presented a theory of the collective modes of the spin-polarized quasi-2D electron gas, showing significant qualitative differences from the unpolarized gas. We believe these results to be applicable to an optically pumped spin-polarized 2D electron gas. In a future communication we hope to examine the questions of the hole plasma, electron-hole coupling, nonzero temperature distributions, and inhomogeneous broadening due to the spatial profile of the pump.

The author wishes to acknowledge many useful conversations with D. Gammon, B. V. Shannabrook, and A. K. Rajagopal. He also wishes to acknowledge the National Research Council for financial support.

[1]T. Ando, J. Phys. Soc. Jpn. **51**, 3893 (1982); A. C. Tselis and J. J. Quin, Phys. Rev. B **29**, 3318 (1984); A. Pinczuk *et al.*, Phys. Rev. Lett. **15**, 1633 (1989).

[2]A. E. Ruckenstein, S. Schmitt-Rink, and R. C. Miller, Phys. Rev. Lett. **56**, 504 (1986).

[3]A. K. Rajagopal, Solid State Commun. **21**, 483 (1977).

[4]A. K. Rajagopal, S. P. Singhal, M. Banerjee, and J. C. Kimball, Phys. Rev. B **17**, 2262 (1978); also see K. M. S. V. Bandara, D. D. Coon, and Byungsung O, Superlatt. Microstruct. **7**, 51 (1990) for an examination of finite width in the Hartree-Fock approximation.

[5]R. O. Jones and O. Gunnarsson, Rev. Mod. Phys. **61**, 689 (1989).

[6]D. Gammon, B. V. Shannabrook, J. C. Ryan, and D. S. Katzer, Phys. Rev. B **41**, 12 311 (1990).

[7]A. K. Rajagopal, Phys. Rev. B **17**, 2980 (1978).